Polym. Bull. (2012) 69:955–965
DOI 10.1007/s00289-012-0806-y

ORIGINAL PAPER

Effects of crystallization condition of poly(ethylene succinate) on the crystallization of poly(ethylene oxide) in their blends

Haijun Wang · Tingshan Zhao · Xuechuan Wang · Peiying Guo · Longfang Ren · Taotao Qiang · Xiaomin Luo · Xihuai Qiang

Received: 21 March 2012 / Revised: 25 June 2012 / Accepted: 6 July 2012 /
Published online: 15 July 2012

Abstract The effects of the crystallization temperatures of poly(ethylene succinate) (PES) on the crystallization behavior of poly(ethylene oxide) (PEO) in their blends were investigated by means of differential scanning calorimetry, atomic force microscopy, and laser confocal fluorescent microscopy. It was found that confined and fractional crystallization of PEO takes place in the PES/PEO blends at all blend ratios if PES is crystallized at higher crystallization temperatures. And morphological observation gives a direct evidence of the different location distribution of PEO, resulting in the confined and fractional crystallization behavior.

Keywords Blends · Crystallization · AFM

Introduction

Blending one polymeric material with another, as a means of developing new polymeric materials with desirable property combinations, is of great scientific and industrial concern. The structure control of polymer blends is essential for improving their macroscopic properties. Binary polymer systems may be of crystalline/crystalline, crystalline/amorphous, and amorphous/amorphous blend types [1–3]. In the crystalline/crystalline polymer blend system, the different crystallization processes of the two components will probably lead to the systems existing in a wide variety of morphological patterns. During the crystallization process of the component with high melting temperature, the other melted component may be expelled into interlamellar, interfibrillar, or interspherulitic domains. Some domains contain various heterogeneities, but some do not contain any of them. Thus, the

H. Wang (✉) · T. Zhao · X. Wang · P. Guo · L. Ren · T. Qiang · X. Luo · X. Qiang
Key Laboratory of Chemistry and Technology for Light Chemical Industry, Ministry of Education, Shaanxi University of Science and Technology, Xi'an 710021, Shaanxi, People's Republic of China
e-mail: wanghaijun@sust.edu.cn

component with low melting temperature crystallizes at different temperatures, which is called fractional crystallization [4].

The fractional crystallization phenomenon occurs mainly in an immiscible blend or a microphase-separated block copolymer. If a semicrystalline polymer is finely dispersed in isolated domains whose number exceeds the number of heterogeneities, the fractional crystallization process can arise [5, 6]. Overviews of fractional crystallization phenomena in a variety of immiscible polymer blends have been given by Frensch et al. [7]. Recently, the confined and fractional crystallization of miscible polymer blends has also attracted much attention. It has been reported that fractional crystallizations occur in the binary blends, such as poly(vinylidene fluoride) (PVDF)/poly(butylene adipate) (PBA) [8] and PBS/poly(ethylene oxide) (PEO) blend [9]. It is to be noted that much of the evidence toward the fractional crystallization in immiscible or miscible blend systems comes from scattering and fairly rudimentary microscopy studies. However, there are only few reports of controlled scanning probe microscopy such as atomic force microscopy (AFM).

The crystallization capacity of a polymer is influenced significantly by the different position in the multi-polymer system. In particular, if this polymer is located in the spatially limited regions inside the spherulites of another polymer, the nucleation and crystal growth of this polymer will be hindered by the pre-existing lamellae or lamellar bundles. To increase our understanding of the internal structure of multipolymer systems, one needs techniques that provide spatial resolution on various length scales within the surface layer and also provide sufficient depth resolution. Klapper and co-workers [10, 11] have investigated the 3D structure of PEO particles in its blend with PE using laser confocal fluorescent microscopy (LCFM), suggesting LCFM can be considered as an alternative method to electron microscopy to visualize the internal structure of polymer blends. The advantage of LCFM is that only light from a particular focal plane reaches the detector. This provides the information from a specific level of the specimen, eliminating contribution of light from adjacent layers. Imaging slices at different depths below the surface of the material enables one to investigate its inner structure. So in this paper, LCFM was applied to determine the location of PEO in PES/PEO blend, which strongly affects the crystallization behavior of PEO.

Qiu and co-workers [12] have studied the effects of blend composition and crystallization temperature on crystalline morphologies of miscible PES/PEO blends using optical microscopy. However, this paper aims to probe confined and fractional crystallization behavior in PES/PEO blend. In the study, the effects of the blend composition and the crystallization temperature of PES on the crystallization behavior and local distribution of PEO in the PES/PEO blend were demonstrated. DSC results reveal that the crystallization behavior of PEO in the PES/PEO blends is greatly affected by the crystallization condition of PES. However, the effect of the blend ratios on the crystallization behavior of the PEO in a PES/PEO blend is significantly different from that in the PBS/PEO blend [9]. Most importantly, the morphological investigation with AFM and LCFM was performed to explain the origin of the fractional crystallization and confirm the morphological detail which fewer direct methods have suggested.

Experimental

Materials and methods

Both PEO (M_w = 100,000 g/mol) and PES (M_w = 200,000 g/mol) were obtained from Aldrich Chemical Company. The melting points of PEO and PES were measured to be 65 and 103 °C, respectively. The labeled poly(ethylene glycol) (PEG)-functionalized $CdSe_{core}$ sample for the observation by fluorescence microscope was synthesized according to the method reported in Ref. [13]. Blends of PES and PEO were prepared by solution blending with chloroform as a common solvent. Both were dissolved in chloroform with desired mass proportions. PES/PEO blends were prepared with various compositions ranging from 100/0, 80/20, 70/30, 60/40, 50/50, 40/60, 30/70, 20/80, to 0/100 in weight ratio, the first number referring to PES.

Experimental procedure

Differential scanning calorimetry (DSC) runs were performed on a Mettler DSC under ultrapure nitrogen purge with 5 mg samples encapsulated in aluminum DSC pans. Tapping-mode AFM images were obtained using a NanoScope III MultiMode AFM (Digital Instruments). The scan rate varied from 0.7 to 1.2 Hz. The scanning density was 512 lines/frame. The experimental details of our high-temperature AFM work can also be found elsewhere [14]. The fluorescent images were taken with an Olympus confocal laser scanning microscope (model Fluoview) specially designed for fluorescence measurement and 3D imaging. For excitation of the fluorescent dye, the 488 nm line of an argon laser was used. A Spatial resolution of approximately 200 and 400 nm axially could be achieved.

Results

Crystallization behavior of PEO

The PES/PEO blends were first melted at 150 °C for 5 min to erase the thermal history, then cooled to the present isothermal crystallization temperatures of PES ($T_{IC,PES}$ = 45–75 °C), and held long enough to complete the crystallization of PES; after that, the blends were cooled to −50 °C at a scanning rate of 10 °C/min followed a holding at −50 °C for 5 min; Finally the samples were heated to 130 °C at a scanning rate of 10 °C/min. The DSC cooling curves after the crystallization of PES are summarized in Fig. 1 for PES/PEO 80/20 (Fig. 1a), 60/40 (Fig. 1b), and 30/70 (Fig. 1c) blends. All the crystallization peaks in Fig. 1 are related to PEO. As shown in Fig. 1a, for the PES/PEO 80/20 blend, a single crystallization peak of PEO appears at about 22 °C when PES crystallizes at a low temperature (e.g. 45 °C). This crystallization peak shifts to a lower temperature and the area of the crystallization exothermic peak decreases with the increase of $T_{IC,PES}$ simultaneously. When $T_{IC,PES}$ is above 65 °C, two crystallization peaks of PEO can be

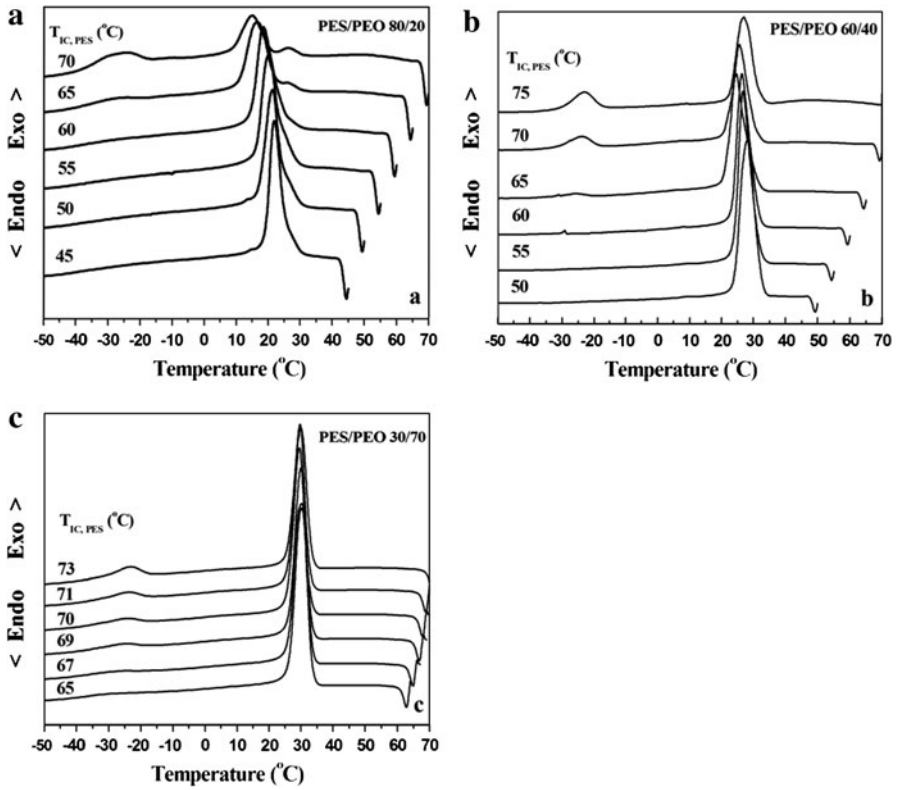

Fig. 1 DSC cooling curves of PES/PEO blends with different blend ratios after being isothermally crystallized at different temperatures (**a** 80/20, **b** 60/40, **c** 30/70). Cooling rate 10 °C/min

observed, suggesting the occurrence of fractional crystallization. The similar phenomena can also be observed in the blends with middle and high PEO content (60/40 and 30/70). Furthermore, the comparison of the positions of the main crystallization peaks in 80/20, 60/40, and 30/70 blends suggests that the blend ratio has some effects on the crystallization behavior of PEO.

Melting behavior of PES/PEO blend

The subsequent melting behavior of PES/PEO blend was then studied at 10 °C/min after the crystallization process as shown in Fig. 1. The DSC heating curves were plotted in Fig. 2 for a PES/PEO 80/20 blend as a function of $T_{IC,PES}$. Two main melting endotherms are found for the PES/PEO 80/20 blend, corresponding to the T_ms of PES and PEO, respectively. It appears that the melting peaks of PES are sensitive to the change of $T_{IC,PES}$ but those of PEO are not. Besides, multiple melting behavior of PES in PES/PEO (80/20) blend is found at all temperatures. This has been reported in different literatures [15–17]. The melting behavior of PEO

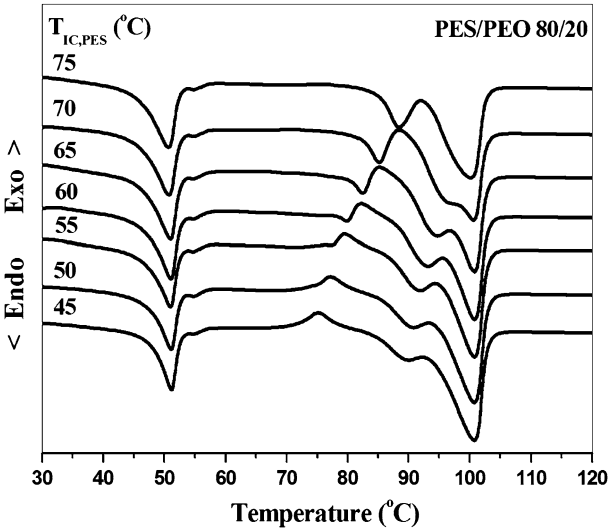

Fig. 2 DSC heating curves (10 °C/min) for PES/PEO (80/20) blends with the PES crystallized at various temperatures and then cooled at a rate of 10 °C/min to −50 °C

or PES in more PEO-concentrated PES/PEO blends shows the same features as does the 80/20 blend.

Morphological structure in the PES/PEO blends

For a better understanding of the morphological details of the PES/PEO blend systems, the morphologies of neat PES and PEO were first examined by atomic force microscopes. In the study of PES/PEO blends, PES crystallizes first, providing the scaffold on which PEO crystallizes. Conveniently, the PES films of the thickness used here can be crystallized with the PES platelets viewed either face-on or edge-on, depending on $T_{IC,PES}$.

Figure 3 shows PES films crystallized isothermally at (a, b) 80 °C, (c) 65 °C, and (d) 50 °C, respectively. When crystallized at 80 °C, PES forms face-on lamelliform crystals in the plane of the film; at 65 °C, PES still exhibits fundamentally face-on morphology with an irregular shape, but with many crystals rotating into an edge-on orientation; however, it appears basically as an edge-on morphology at 50 °C. In our previous work, the morphology of neat PEO has been investigated, which is similar to that of PES [14]. At small supercooling, the crystals seen face-on are formed in the plane of the film. At large supercooling, the edge-on lamellae have their face normals in the plane of the film.

To investigate the fine structure of the PES/PEO blend, we chose a PES/PEO 50/50 blend at different $T_{IC,PES}$ as a specimen. To find out the exact location of the PEO crystals, the fine structure of the blend was examined using AFM. Figure 4 shows AFM phase images of a 50/50 blend in which PES was isothermally crystallized at 50 °C prior to cooling the film to 25 °C. Figure 4a was scanned at

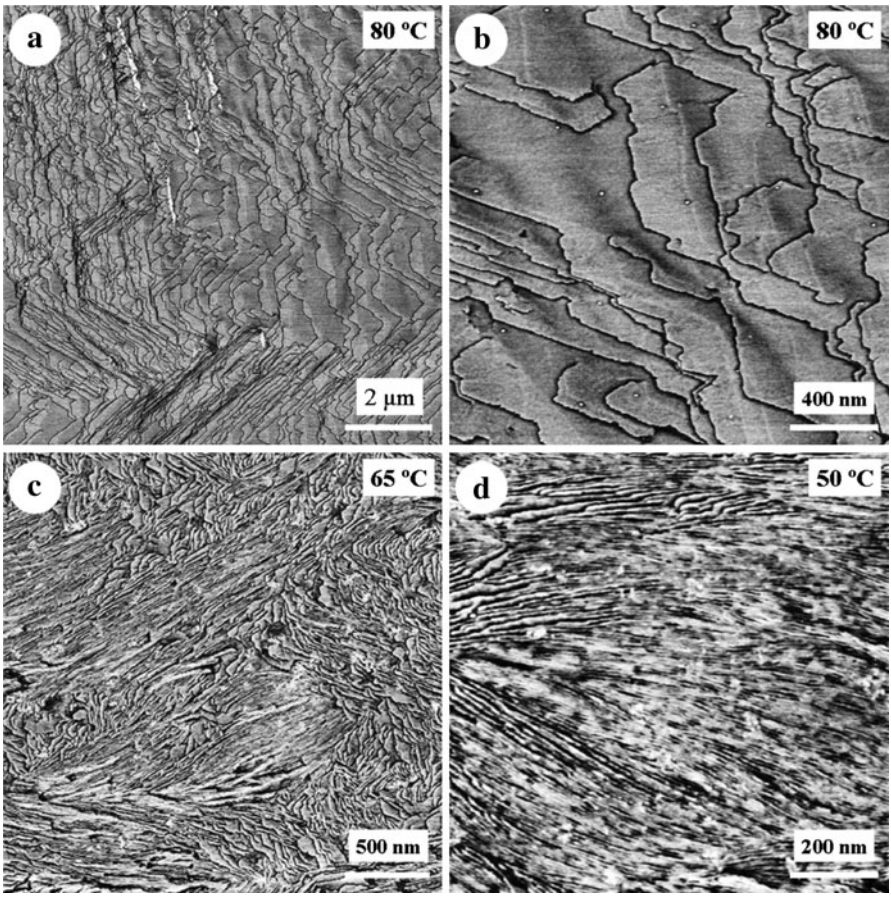

Fig. 3 AFM morphologies of PES at different crystallization temperatures (**a**, **b** 80 °C, **c** 65 °C, **d** 50 °C)

25 °C, while Fig. 4b at 65 °C (well above the melting temperature of PEO, but below the melting temperature of PES). The purpose of heating the sample to 65 °C is to locate PEO, the image of which reflects the PES crystals only. Unlike pure PES (Fig. 3d), PES in the PES/PEO blend forms a scaffold, or lamellar bundles (Fig. 4b), i.e., the increase of PEO content leads to an even sparser arrangement in the PES crystals. Between the lamellar bundles, there exist narrow interbranch pockets filled with the melted PEO. When the temperature is below the melting point of PEO, PEO then crystallizes in the regions between the existing lamellar bundles of PES (Fig. 4a).

Figure 5 shows the AFM phase image of a 50/50 PES/PEO blend with the PES crystallized at 80 °C and then cooled to 0 °C. As in the case of pure PES crystallized at 80 °C, PES in the PES/PEO 50/50 blend forms flat-on crystals, on which patches of edge-on PEO lamellae can be seen. However, in the region shown in Fig. 5, the total area covered by the crystalline PEO is evidently less than the overall composition. Other regions show no more than this level of PEO coverage.

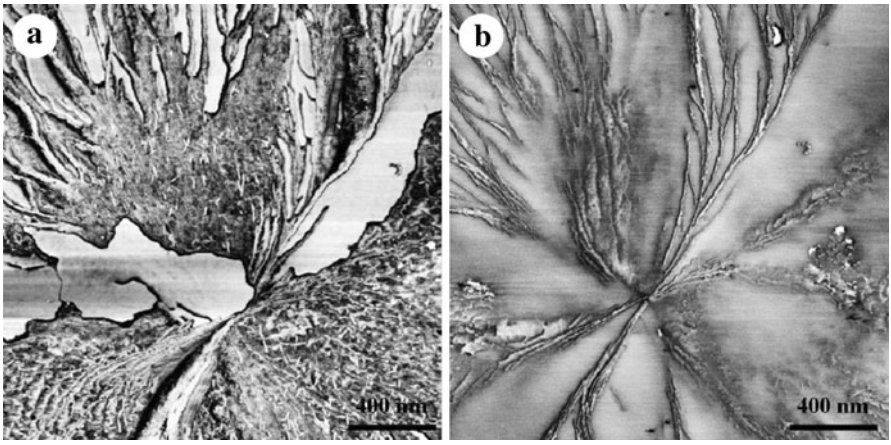

Fig. 4 AFM phase images of a 50/50 PES/PEO blend with the PES crystallized at 50 °C and then cooled to 25 °C. The images were scanned at 25 °C (**a**) and 65 °C (**b**), respectively

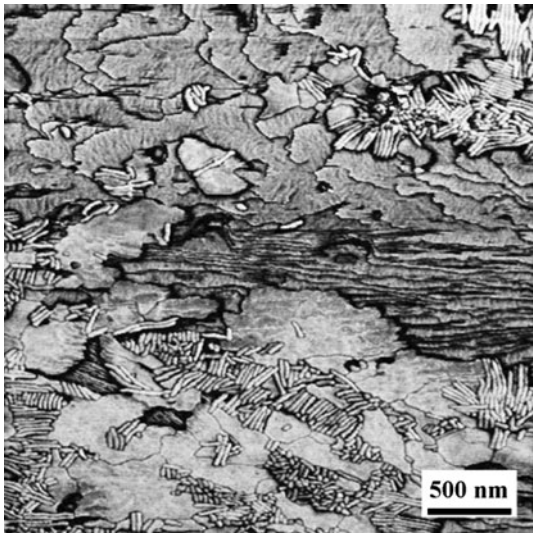

Fig. 5 AFM phase images of a 50/50 PES/PEO blend with the PES crystallized at 80 °C and then cooled to 0 °C. The image was scanned at 25 °C

Therefore, the remaining PEO was presumably below the surface, probably between PES lamellae.

To investigate the internal structure of the PES/PEG-CdSe 50/50 blend with the PES crystallized at 80 °C, the sample was imaged by LCFM. The sample was sliced up into several planes so that its three full dimensional structure could be obtained. As is shown in Fig. 6, optical slicing was carried out at an interval of every 4 μm distance for a section smaller than this can not provide any additional information. The PEG-CdSe domains appear red against the dark PES background, which is helpful to distinguish two components. As shown in Fig. 6a, there is some PEO expelled onto the surface of the PES spherulites, which is consistent with the AFM

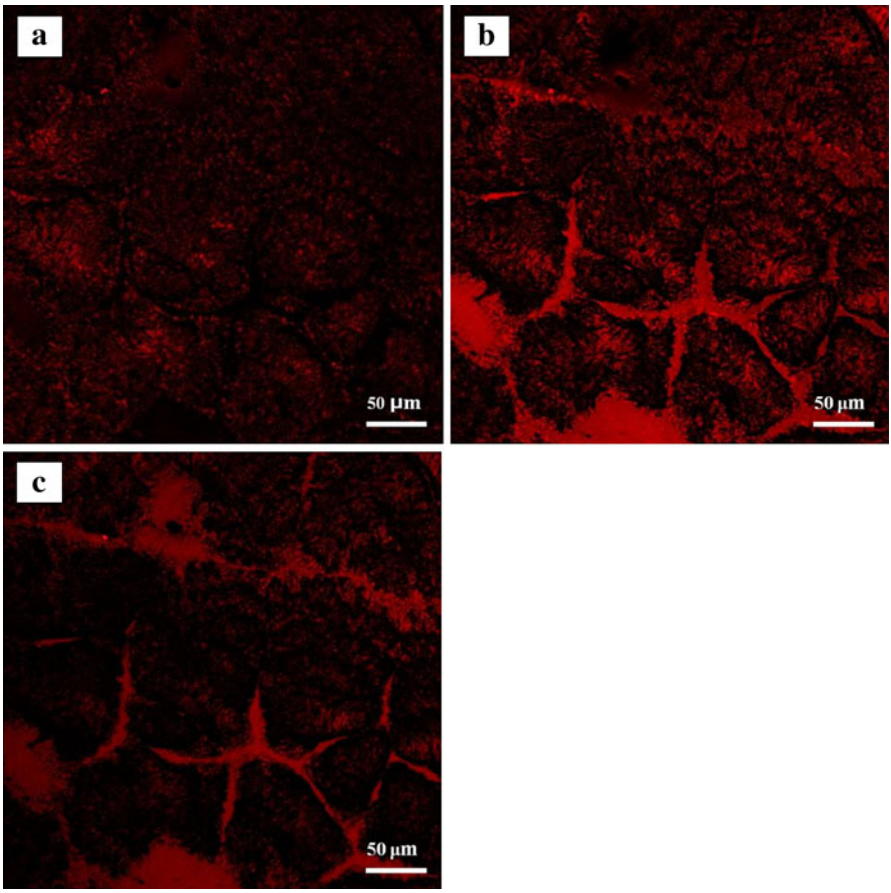

Fig. 6 LCFM images of a 50/50 PES/PEO blend with the PES crystallized at 80 °C and then cooled to 0 °C. Image **a** the film surface, **b** a slice 4 μm beneath the surface, and **c** a slice 8 μm beneath the surface

results. Figure 6b, c shows the imaging slice at 4 and 8 μm deep beneath the surface. It was found that some of PEO are embedded into the interlamellar or interfibrillar regions of PES spherulites, while the rest of PEO appear in the interspherulitic regions of PES spherulites. It should be noted that the resolution of LCFM is limited by the laser wavelength, a factor of 50 lower than for electron microscopy or AFM. As a result, it is hard to exactly locate PEO in PES spherulites, e.g., interlamellar or interfibrillar regions.

Discussion

The DSC results have revealed that the isothermal crystallization temperature of PES ($T_{IC,PES}$) significantly affects the crystallization behavior of PEO (Fig. 1). If PES isothermally crystallizes at 70 °C or higher in the PES/PEO blends with

different blend ratios, two crystallization peaks of PEO will be detected. Most of PEO crystallizes at 30 °C while the rest of PEO crystallizes at about −25 °C, suggesting the occurrence of fractional crystallization. It was further found that, with the increment of $T_{IC,PES}$, the areas of the major crystallization peaks of PEO at 30 °C become smaller, while those at −25 °C are increased, suggesting that the morphology formed at comparatively higher $T_{IC,PES}$ will affect the crystallization ability of PEO, consequently leading to failure of PEO crystallization at normal temperature.

Based on AFM and LCFM observation results, it is easy to understand the above fractional crystallization behavior of PEO in the PES/PEO blend. During the PES crystal growth, crystallization is accompanied with the segregation of the temporary amorphous PEO. When crystallized at high temperature, PES form the flat-on lamellae, to the surface of which a major portion of PEO will be expelled. This part of PEO, not confined in minor phase, therefore shows the crystallization behavior similar to the bulk polymer. When the temperature reduced to 0 °C, PEO expelled to the surface form edge-on crystals. The total area covered by these crystals is obviously smaller than the overall composition, indicating that a small portion of PEO probably resides in the PES interlamellar spaces. As the space between the PES lamellae is only several nanometer, the number of PEO microphase-separated domains is of the same order of magnitude or even greater than the number of usually active heterogeneities [17]. As a result, the crystallization of this part of PEO is basically induced by much less active heterogeneities or homogeneous nucleation at extreme supercooling. When crystallized at low temperature, PES forms edge-on lamellar bundles, which is quite different from the case of high temperature. During the PES crystallization the entire melted PEO is expelled into the interfibrillar regions ranging from tens to hundreds of nanometers, so that the crystallization of PEO is induced by active heterogeneous nucleation.

It has been reported that the phase separation in crystalline blends during the crystallization of one component can be understood in terms of the diffusion length $\delta = D/G$, where D is the diffusion coefficient of the noncrystallizable species in the blend and G is the radial growth rate of the spherulites. In our previous work, the morphologies of poly(butylene succinate) (PBS)/poly(butylene adipate) (PBA) blends with different blend ratios and crystallization processes have been investigated [18]. The results show that interspherulitic phase segregation of PBA takes place at high temperature for all compositions due to the high diffusion length. Thus, for the PES/PEO blends, the positional distribution of PEO during the crystallization of PES predicted from δ should have been as follows: higher $T_{IC,PES}$ favors the expelling of PEO from the interlamellar region, while lower $T_{IC,PES}$ contributes to the remaining of PEO in the interlamellar region, which contradicts the experimental results.

Interestingly, the fractional crystallization of PEO in our experiment has also been observed in the PBS/PEO blend [9]. The difference between the PBS/PEO and PES/PEO blend systems lies in how well the blend ratio affects the crystallization of PEO in PBS/PEO blends, the confined and fractional crystallization of PEO can be observed in PBS-rich blend regardless of the crystallization temperature of PBS. For the PES/PEO blend, however, the blend ratios have nothing to do with the fractional

crystallization of PEO. Anyway, as to the mechanism and essence of phase segregation of PEO during the crystallization of PES the further investigation is expected.

Conclusions

The effects of the crystallization temperatures of poly(ethylene succinate) (PES) on the crystallization behavior of poly(ethylene oxide) (PEO) in their blends have been investigated by DSC, LCFM, and AFM. It was found that the crystallization behavior of PEO in PES/PEO blends is significantly affected by the crystallization temperature of PES. When PES is crystallized at high crystallization temperatures, confined, and fractional crystallization of PEO occurs in the PES/PEO blends at all blend ratios. Morphological observation gives a direct evidence of the different location distribution of PEO, resulting in the confined and fractional crystallization behavior. The fractional crystallization of PEO arises from one portion of PEO included in the interlamellar region while the other excluded from the interlamellar region.

Acknowledgments The financial support by Natural Science Basic Research Plan in Shaanxi Province of China (Program No. 2011JQ2004), National Natural Science Foundations of China (21076120), Scientific Research Program Funded by Shaanxi Provincial Education Department (Program No. 11JK0576), Scientific Research Foundation of Shaanxi University of Science and Technology (No. BJ11-08) and Natural Science Basic Research Plan in Zhejiang Province of China (Program No. 2011C31004) are gratefully acknowledged.

References

1. Kowalewski T, Ragosta G, Martuscelli E, Galeski A (1997) Crystallization of poly(ethylene oxide) in i-polypropylene-poly(ethylene oxide) blends. J Appl Polym Sci 66:2047–2057
2. Molinuevo CH, Mendez GA, Müller AJ (1998) Nucleation and crystallization of PET droplets dispersed in an amorphous PC matrix. J Appl Polym Sci 70(9):1725–1735
3. Arnal ML, Müller AJ (1999) Fractionated crystallisation of polyethylene and ethylene/α-olefin copolymers dispersed in immiscible polystyrene matrices. Macromol Chem Phys 200(11):2559–2576
4. Arnal ML, Müller AJ, Maiti P, Hikosaka M (2000) Nucleation and crystallization of isotactic poly(propylene) droplets in an immiscible polystyrene matrix. Macromol Chem Phys 201(17): 2493–2504
5. Müller AJ, Arnal ML, López-Carrasquero F (2002) Nucleation and crystallization of PS-*b*-PCL triblock copolymers. Macromol Symp 183(1):199–204
6. Arnal ML, Balsamo V, Lopez-Carrasquero F, Contreras J, Carrillo M, Schmalz H, Abetz V, Laredo E, Müller AJ (2001) Synthesis and characterization of polystyrene-*b*-poly(ε-caprolactone) block copolymers. Macromolecules 34(23):7973–7982
7. Frensch H, Harnischfeger P, Jungnickel BJ (1989) In: Utracki LA, Weiss RA (eds) Multiphase polymers: blends and ionomers. ACS Symposium Series, vol 395, p 101. American Chemical Society: Washington, DC
8. Yang JJ, Pan PJ, Hua L, Zhu B, Dong T, Inoue Y (2010) Polymorphic crystallization and phase transition of poly(butylene adipate) in its miscible crystalline/crystalline blend with poly(vinylidene fluoride). Macromolecules 43(20):8610–8618
9. He Y, Zhu B, Kai WH, Inoue Y (2004) Effects of crystallization condition of poly(butylene succinate) component on the crystallization of poly(ethylene oxide) component in their miscible blends. Macromolecules 37(21):8050–8056

10. Jang YJ, Bieber K, Naundorf C, Nenov N, Klapper M, Müllen K, Ferrari D, Knoke S, Fink G (2005) Optical methods to study the behaviour of supported metallocene catalysts during olefin polymerisation. e-Polymers 013:1–13
11. Jang YJ, Naundorf C, Klapper M, Müllen K (2005) Study of the fragmentation process of different supports for metallocenes by laser scanning confocal fluorescence microscopy (LSCFM). Macromol Chem Phys 206(20):2027–2037
12. Lu JM, Qiu ZB, Yang WT (2008) Effects of blend composition and crystallization temperature on unique crystalline morphologies of miscible poly(ethylene succinate)/poly(ethylene oxide) blends. Macromolecules 41(1):141–148
13. Dubavik A, Lesnyak V, Thiessen W, Gaponik N, Wolff T, Eychmüller A (2009) Synthesis of amphiphilic CdTe nanocrystals. J Phys Chem C 113(12):4748–4750
14. Wang HJ, Schultz JM, Yan S (2007) Study of the morphology of poly(butylene succinate)/poly(ethylene oxide) blends using hot-stage atomic force microscopy. Polymer 48(12):3530–3539
15. Qiu ZB, Komura M, Ikehara T, Nishi T (2003) DSC and TMDSC study of melting behavior of poly(butylene succinate) and poly(ethylene succinate). Polymer 44(26):7781–7785
16. Yasuniwa M, Satou T (2002) Multiple melting behavior of poly(butylene succinate). I. Thermal analysis of melt-crystallized samples. J Polym Sci, Polym Phys 40(21):2411–2420
17. Gan ZH, Abe H, Doi Y (2000) Biodegradable poly(ethylene succinate) (PES). 1. Crystal growth kinetics and morphology. Biomacromolecules 1(4):704–712
18. Wang HJ, Gan ZH, Schultz JM, Yan SK (2008) A morphological study of poly(butylene succinate)/poly(butylene adipate) blends with different blend ratios and crystallization processes. Polymer 49(9):2342–2353